J Gynecol Oncol. 2022 Jan;33(1):e7
https://doi.org/10.3802/jgo.2022.33.e7
pISSN 2005-0380·eISSN 2005-0399

JOURNAL OF GYNECOLOGIC ONCOLOGY

Original Article

A novel gene signature associated with poor response to chemoradiotherapy in patients with locally advanced cervical cancer

Kyung Hwan Kim, Jee Suk Chang, Hwa Kyung Byun, Yong Bae Kim

Department of Radiation Oncology, Yonsei Cancer Center, Yonsei University College of Medicine, Seoul, Korea

Received: May 1, 2021
Revised: Sep 6, 2021
Accepted: Oct 5, 2021

Correspondence to
Yong Bae Kim
Department of Radiation Oncology, Yonsei Cancer Center, Yonsei University College of Medicine, 50-1 Yonsei-ro, Seodaemun-gu, Seoul 03722, Korea.
E-mail: ybkim3@yuhs.ac

ORCID iDs
Kyung Hwan Kim
https://orcid.org/0000-0002-6713-1350
Jee Suk Chang
https://orcid.org/0000-0001-7685-3382
Hwa Kyung Byun
https://orcid.org/0000-0002-8964-6275
Yong Bae Kim
https://orcid.org/0000-0001-7573-6862

Funding
This study was supported by a faculty research grant of Yonsei University College of Medicine (6-2021-0098).

ABSTRACT

Objective: We aimed to investigate the distinct transcriptional landscape in poor responders to concurrent chemoradiotherapy (CCRT) and to gain mechanistic insights into treatment resistance in cervical cancer.
Methods: RNA sequencing was performed in patients with locally advanced cervical cancer treated with platinum-based CCRT. Transcriptome data of no durable benefit (NDB; progression-free period <3 years) and durable clinical benefit (DCB; progression-free period >5 years) patients were compared. The NDB score was estimated for each patient using differentially expressed genes between NDB and DCB patients. The potential response to programmed death-1 blockade was estimated using the tumor immune dysfunction and exclusion (TIDE) score and T-cell-inflamed gene expression profile (GEP).
Results: NDB patients exhibited a distinct transcriptional profile compared to DCB patients, such as higher signatures of extracellular matrix organization and epithelial-to-mesenchymal transition. The fraction of cancer-associated fibroblasts (CAFs) within the tumor was significantly higher in NDB patients than in DCB patients. High NDB scores were significantly associated with poor survival in the Cancer Genome Atlas cervical cancer cohort (n=274; p=0.015) but only in patients who received curative aim radiotherapy (p=0.002). Patients with high NDB scores displayed significantly higher TIDE prediction scores and lower T-cell-inflamed GEP scores than those with low NDB scores.
Conclusion: Patients with cervical cancer having poor CCRT or RT outcomes exhibited a distinct gene signature that could predict treatment outcomes. For poor responders, immune checkpoint inhibitors may be less effective whereas CAF-targeting treatments may be a promising approach.

Keywords: Cervical Cancer; Chemoradiotherapy; Gene Signature; Cancer-associated Fibroblasts

Synopsis

- A subgroup of patients with locally advanced cervical cancer exhibit no durable benefit (NDB) after chemoradiotherapy.
- NDB patients exhibited a distinct transcriptional profile
- NDB signature score predicted poor outcome in independent cohorts.
- NDB patients may have poor response to immune checkpoint blockade.

Conflict of Interest
No potential conflict of interest relevant to this article was reported.

Author Contributions
Conceptualization: K.K.H., K.Y.B.; Data curation: K.K.H., C.J.S., B.H.K.; Formal analysis: K.K.H.; Investigation: K.K.H., C.J.S., B.H.K., K.Y.B.; Methodology: K.K.H.; Supervision: C.J.S., K.Y.B.; Visualization: K.K.H.; Writing - original draft: K.K.H.; Writing - review & editing: K.K.H., C.J.S., B.H.K., K.Y.B.

INTRODUCTION

Cervical cancer is the fourth most commonly diagnosed cancer and the fourth leading cause of cancer-related deaths among women worldwide [1]. Despite the decreasing proportion of cervical cancer due to effective screening and vaccination programs, the incidence and mortality rates of cervical cancer are still considerably higher in transitioning countries [1]. Most early-stage cervical cancers are cured by surgical resection. For locally advanced diseases, concurrent chemoradiotherapy (CCRT) is the treatment of choice [2-4]. However, even with modern radiation techniques, 30% of patients with locally advanced cervical cancer experience treatment failure after curative aim CCRT [5,6].

To overcome the limitations of current standard treatment, adjuvant or neoadjuvant chemotherapy, immune checkpoint inhibitors (ICIs), and other target agents are under investigation [7]. Although the results of OUTBACK (NCT01414608) and INTERLACE (NCT01566240) are awaited, additional chemotherapy with standard CCRT has shown conflicting results [8-10]. The results of the combination of ICIs with CCRT have only been reported in early clinical trials [11], and several phase III trials are currently under investigation [12]. Most of these trials focused on treatment intensification in patients with locally advanced cervical cancer without applying relevant biomarkers for patient selection. To better define optimal candidates for treatment intensification, biomarkers that identify patients more likely to fail after CCRT are needed. Moreover, biomarker-driven targets for novel treatment combinations are required.

Gene sets, comprising multiple genes, have been utilized to predict outcomes and guide further treatment. The most popular gene panel used in clinical practice is Oncotype Dx in patients with breast cancer. It is used to select the patient subpopulation that may best fit adjuvant chemotherapy [13]. For radiotherapy (RT), gene-expression-based scoring systems have been proposed but have not been integrated into routine clinical practice [14,15]. These gene sets are either derived from cancer cell lines [14], which do not consider tumor microenvironment factors, or developed in postoperative settings [15]. Moreover, no specific gene set has been suggested to predict the response to CCRT in patients with cervical cancer. In the present study, we aimed to identify a distinct gene expression signature associated with poor treatment outcomes and to gain mechanistic insights into treatment resistance in a subpopulation of patients with early treatment failure.

MATERIALS AND METHODS

1. Patients and treatment

Patients with pathologically confirmed locally advanced uterine cervical cancer who received definitive CCRT or RT were included in the study. Among 679 patients that received definitive CCRT or RT between January 1995 and August 2012, 528 patients were available for formalin-fixed paraffin-embedded (FFPE) tissues. Among the 528 patients, 26 patients had recurrence within 36 months (no durable benefit [NDB]) and 403 patients had no recurrence or recurrence after 60 months (durable clinical benefit [DCB]; **Fig. 1**). From our previous reports, recurrences were mostly evident before 36 months and rare after 60 months [6,16]. Propensity score matching was performed to adjust the imbalance of baseline characteristics between NDB and DCB patients (**Table S1**). In total, four patients with NDB and five patients with DCB were included for RNA sequencing. The details of RT and chemotherapy

https://doi.org/10.3802/jgo.2022.33.e7

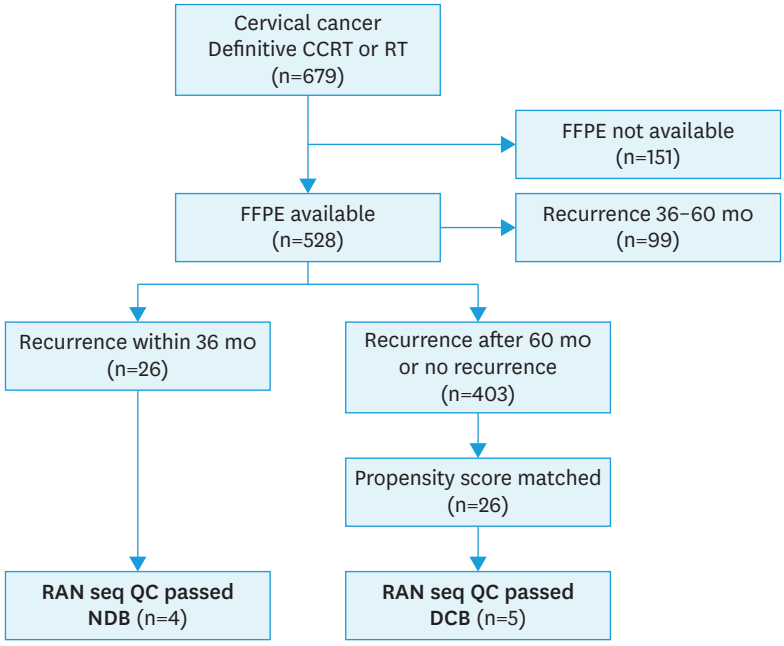

Fig. 1. CONSORT diagram of the patients analyzed in the present study.
CCRT, concurrent chemoradiotherapy; FFPE, formalin-fixed paraffin-embedded; NDB, no durable benefit; RT, radiotherapy; QC, quality control.

have been described previously [16]. In brief, RT consisted of external beam radiotherapy (EBRT) at 45 Gy in 25 fractions covering the whole pelvis and high-dose-rate intracavitary brachytherapy (HDR-ICBT) at 30 Gy in 6 fractions. The chemotherapy regimen used was a combination of cisplatin or carboplatin with 5-fluorouracil administered every 3 weeks or a weekly administration of cisplatin or carboplatin. Follow-up examinations, which included physical examinations, computed tomography, and magnetic resonance imaging, were performed every 3 months for the first 2 years, every 6 months for the next 3 years, and once per year thereafter. The study was conducted according to the guidelines of the Declaration of Helsinki and was approved by the Institutional Review Board of Severance Hospital (4-2015-0454), which also waived the need to obtain informed consent due to the retrospective nature of this study.

2. Tumor tissue preparation

RNA was extracted from FFPE tissue sections with an RNeasy FFPE Kit (Qiagen, Hilden, Germany), and only samples that passed the quality control tests were further processed for RNA sequencing. RNA quality was assessed using an Agilent 2100 Bioanalyzer and an RNA 6000 Nano Chip (Agilent Technologies, Palo Alto, CA, USA), and RNA quantification was performed using an ND-2000 Spectrophotometer (Thermo Fisher Scientific, Waltham, MA, USA). In total, four NDB patients and five DCB patients who had sufficient amounts of RNA and had passed quality assessments underwent RNA sequencing.

3. RNA sequencing and analysis

An oligo-dT primer containing an Illumina-compatible sequence at its 5' end was hybridized to the RNA for reverse transcription. After degradation of the RNA template, second-strand synthesis was initiated with a random primer containing an Illumina-compatible linker sequence at its 5' end. The double-stranded library was purified using magnetic beads. The

https://doi.org/10.3802/jgo.2022.33.e7

library was amplified to add the adapter sequences required for cluster generation. Purified libraries were sequenced using HiSeq 2500 (Illumina) at an average of 58 million paired-end 100-bp reads. Reads were aligned to the human genome (hg19) using TopHat v2.1.1. The number of mapped reads for each gene was quantified using the StringTie. Gene counts were normalized by library size, and the differential expression of genes was analyzed using DESeq2 (v.1.24.0). Differentially expressed genes (DEGs) were determined as those with an adjusted $p<0.05$ and a $\log_2$ fold-change >1. Heatmaps were generated using the pheatmap package (v1.0.12). Enriched biological processes and pathways of genes upregulated in NDB and DCB patients were annotated by gene ontology and Kyoto Encyclopedia of Genes and Genomes pathway terms using DAVID [17]. Gene set enrichment analysis (GSEA) was performed using Broad Institute software (http://software.broadinstitute.org/gsea/index.jsp). The curated gene sets of transforming growth factor (TGF)-β response [18], wound healing, epithelial-mesenchymal transition (EMT) [19], and radioresistance [20] were obtained from previous studies. CIBERSORTX was used to analyze the cellular composition of the tumor microenvironment [21]. Due to the lack of data on cervical cancer in this model, we applied the head and neck squamous cell carcinoma tumor-trained model. Gene signatures of cancer-associated fibroblasts (CAFs), tumor-associated macrophages (TAMs), and myeloid-derived suppressor cells (MDSCs) were obtained from previous studies [22-24]. RNA sequencing data are available from the NCBI GEO (GSE168009).

4. NDB score and survival analysis

An "NDB score" was calculated for each individual using gene set variation analysis (GSVA) with the GSVA R package (v.1.32.0) and was defined as the enrichment score for the gene set derived from the DEGs between NDB and DCB tumors. In detail, the GSVA score for significantly downregulated genes in the NDB tumor was subtracted from the GSVA score of significantly upregulated genes in NDB tumors. Patients were dichotomized according to the NDB score as "high" (NDB score >0) and "low" (NDB score <0). We analyzed survival outcomes according to the NDB score in the Cancer Genome Atlas Cervical Squamous Cell and Endocervical Adenocarcinoma (TCGA-CESC) cohort. RNA-sequencing data and patient clinical information from the TCGA database were obtained using FireBrowse (Broad Institute). Furthermore, the predictive value of the NDB score was analyzed according to the receipt of curative aim RT, which was defined as receiving RT but not surgery. In addition, we further validated the predictive value of the NDB score with regard to overall survival in two independent cohorts (GSE39001 and GSE52904) [25,26]. Only patients who received curative aim RT were included in the analysis. Two patients were absent of gene expression data in the GSE39001 data set. NDB and DCB patients in the TCGA data base were divided according to the provided progression-free interval. NDB and DCB patients in the two other cohorts, GSE39001 and GSE52904, were divided according to overall survival since they only provided overall survival data.

5. Predicting the response to anti-programmed death-1 (PD-1) therapy

The T cell-inflamed gene expression profile (GEP) [27], which is known to predict tumor response to anti-PD-1 therapy, was utilized to predict the response to anti-PD-1 therapy. In addition, the recently developed tumor immune dysfunction and exclusion (TIDE) algorithm was used to predict the response to ICIs [28]. In brief, this algorithm estimates a TIDE prediction score for each individual based on gene expression data; a higher TIDE score is associated with a poorer response to ICIs. The neoantigen load for each patient from the TCGA-CESC cohort was obtained from a previous study [18]; it was determined from single-nucleotide variants and indel mutations that were predicted to result in major histocompatibility complex binding peptides.

6. Statistical analysis

The Student's t-test was performed to compare continuous variables between two groups. Survival curves were generated using Kaplan-Meier curves and compared using a log-rank test. Propensity score matching was performed by 1:1 nearest neighbor analysis, with a caliper width of 0.2 standard deviations of the logit distance measured using the R-package, "MatchIt." The covariates used for matching included age, FIGO stage, tumor size, histology, pelvic lymph node involvement, and chemotherapy. Statistical significance was set at $p<0.05$. All statistical analyses were performed using R v3.6.2 (http://www.r-project.org) or GraphPad Prism v6.0 (GraphPad Software Inc., San Diego, CA, USA).

RESULTS

1. Patient characteristics

The characteristics of the four NDB patients and five DCB patients who underwent RNA sequencing are summarized in **Table 1**. Most patients had squamous cell histology, and one patient was diagnosed with adenocarcinoma. All patients received EBRT followed by HDR-ICBT with concurrent chemotherapy. At 3 months post CCRT, eight patients exhibited a clinically complete response, whereas one patient exhibited a partial response and underwent salvage hysterectomy. The median time to progression was 12.6 months in NDB patients, and no recurrences were observed in DCB patients. Among the NDB patients, the first location of recurrence was locoregional in two patients and distant in two patients. The median overall survival was 44 months (95% confidence interval [CI], 5.3–82.7 months) in NDB patients and not reached in DCB patients (p=0.022).

2. The distinct transcriptional profiles in NDB patients

The principal component analysis revealed distinct transcriptional landscapes in NDB and DCB patients (**Fig. 2A**). A total of 185 DEGs were identified, of which 100 genes were significantly upregulated in NDB and 85 genes were significantly upregulated in DCB patients

Table 1. Characteristics of patients with NDB (n=4) and DCB (n=5) that underwent RNA sequencing

Patients	Age	Histology	FIGO Stage*	LN metastasis	Radiotherapy	Chemotherapy	3-mo tumor response	Recur	Time to progression (m)	Survival (m)	Last f/u status
NDB1	28	SCC	IIA2 (IIA2)	None	EBRT 45 Gy + ICBT 24Gy	5-FU + Carboplatin	CR	Lung, mediastinal LNs	7.5	16.5	Dead
NDB2	35	SCC	IIB (IIIC1)	Pelvic LN	EBRT 45 Gy + ICBT 30Gy	Cisplatin	CR	Lung	7.8	69.9	Alive
NDB3	62	SCC	IIB (IIB)	None	EBRT 45 Gy + ICBT 30Gy	5-FU + Cisplatin	CR	Local	17.3	56.0	Dead
NDB4	50	ADC	IIB (IIIC1)	Pelvic LN	EBRT 45 Gy + ICBT 30Gy	Cisplatin	PR	Pelvic LN	26.9	44.0	Dead
DCB1	76	SCC	IIA1 (IIA1)	None	EBRT 45 Gy + ICBT 30Gy	Carboplatin	CR	None	-	72.1	Alive
DCB2	75	SCC	IIB (IIIC1)	Pelvic LN	EBRT 45 Gy + ICBT 30Gy	Carboplatin	CR	None	-	60.8	Alive
DCB3	45	SCC	IB2 (IB3)	None	EBRT 41.4 Gy + ICBT 30Gy	Carboplatin	CR	None	-	72.3	Alive
DCB4	43	SCC	IIB (IIIC1)	Pelvic LN	EBRT 45 Gy + ICBT 30Gy	Cisplatin	CR	None	-	136.2	Alive
DCB5	44	SCC	IIA2 (IIA2)	None	EBRT 45 Gy + ICBT 30Gy	Cisplatin	CR	None	-	169.0	Alive

ADC, adenocarcinoma; CCRT, concurrent chemoradiotherapy; CR, complete response; DCB, durable clinical benefit (PFS >60 months); EBRT; external beam radiotherapy; FIGO, International Federation of Gynecology and Obstetrics; ICBT, intracavitary brachytherapy; LN, lymph node; NDB, no durable benefit (PFS <36 months); OS, overall survival; PFS, progression-free survival; PR, partial response; SCC, squamous cell carcinoma.
*FIGO stage 2009 (FIGO stage 2018).

https://doi.org/10.3802/jgo.2022.33.e7

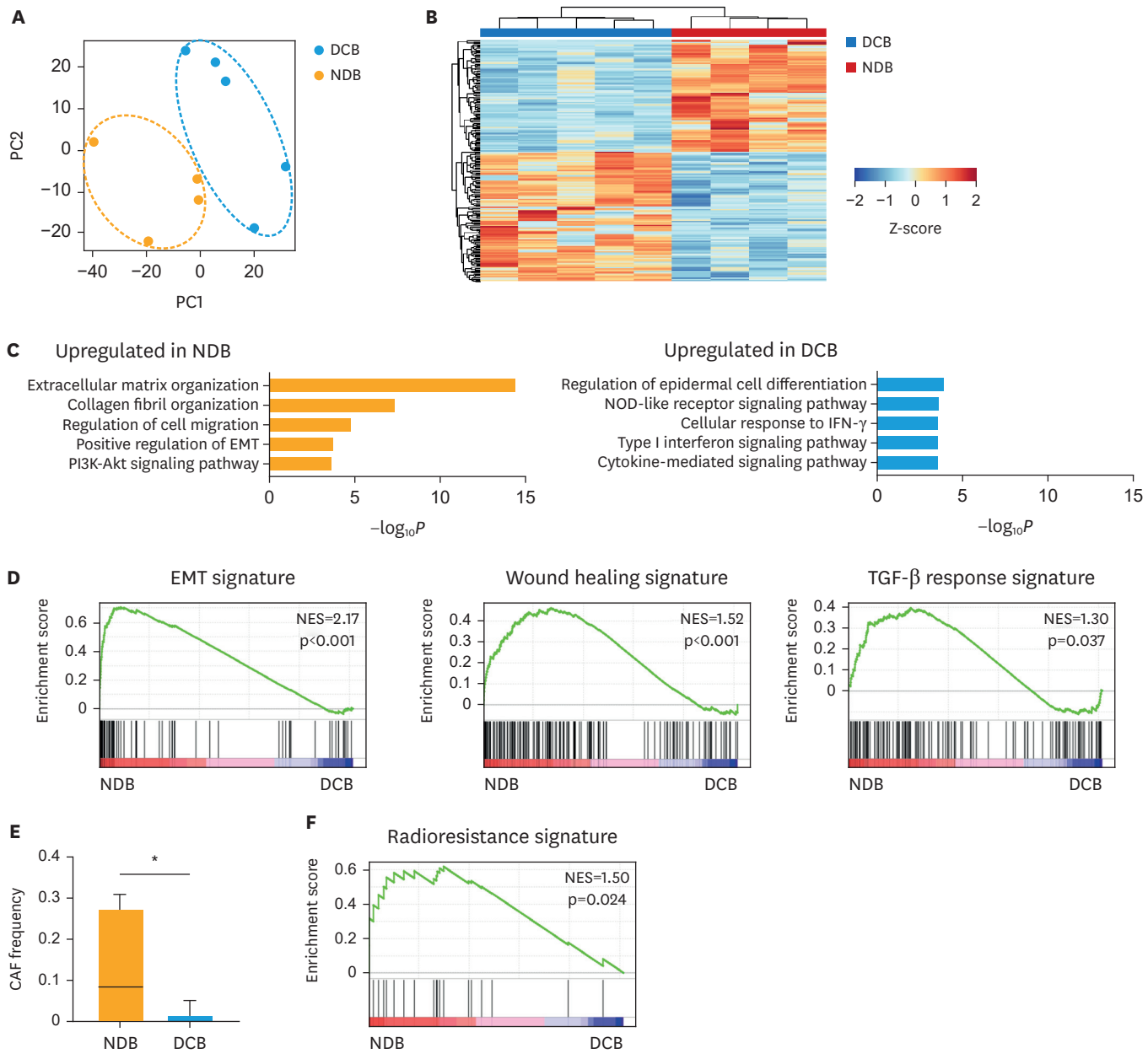

Fig. 2. Transcriptome analysis of DCB (n=5) and NDB (n=4) patients. (A) Principal component analysis of DCB and NDB patients. (B) Hierarchical clustering analysis of differentially expressed genes (log_2 fold change >1, adjusted p<0.05) in DCB and NDB patients. (C) Enriched biological processes and pathways of genes upregulated in NDB and DCB patients. (D) Gene set enrichment analysis regarding EMT signature, wound healing signature, and TGF-β response signature. (E) Frequency of CAFs estimated by CIBERSORTx. (F) Gene set enrichment analysis of a radioresistant gene signature.
CAF, cancer-associated fibroblast; DCB, durable clinical benefit; EMT, epithelial-mesenchymal transition; NDB, no durable benefit; TGF, transforming growth factor.
*p<0.05.

(**Fig. 2B**; **Table S2**). Unsupervised hierarchical clustering confirmed that the gene signatures of NDB and DCB patients were distinct (**Fig. 2B**). Genes upregulated in NDB patients were associated with extracellular matrix (ECM) organization, cell migration, and EMT (**Fig. 2C**). In contrast, genes upregulated in patients with DCB were associated with epidermal cell differentiation and interferon-related pathways (**Fig. 2C**). GSEA also demonstrated significant enrichment of the EMT gene signature in NDB patients (**Fig. 2D**). Other gene signatures related to EMT, such as the wound healing signature and TGF-β response signature, were

https://doi.org/10.3802/jgo.2022.33.e7

JOURNAL OF GYNECOLOGIC ONCOLOGY

also significantly enriched in NDB patients (**Fig. 2D**). Next, we enumerated the frequency of CAFs by deconvolution of bulk RNA-sequencing data using CIBERSORTx. The frequency of CAFs was significantly higher in NDB patients than in DCB patients (**Fig. 2E**). Indeed, NDB patients exhibited a significant enrichment of a radioresistant gene signature (**Fig. 2F**).

3. Predictive role of the NDB score in independent cohorts

Next, we evaluated whether the distinct gene signature of NDB patients could predict treatment outcomes following CCRT in patients with cervical cancer. Using the DEGs between NDB and DCB patients, we could derive an "NDB score" for each patient. First, we utilized the TCGA-CESC cohort (n=273) to test the predictive power of the NDB score. NDB score was significantly higher in NDB patients compared to DCB patients (**Fig. 3A**). In addition, patients with high NDB scores had a significantly lower survival even after adjusting for age, tumor histology, and tumor stage (adjusted hazard ratio 2.02; 95% CI, 1.25–3.26; **Fig. 3A**). Considering that the NDB score is derived from a cohort of patients who received curative aim CCRT, we evaluated the predictive role of the NDB score in subgroups of patients who did or did not receive curative aim RT. The NDB score predicted poor outcomes only in the subgroup of patients who received curative aim RT (**Fig. 3B**) and not in patients who did not receive curative aim RT (**Fig. 3C**). We further tested the prognostic value of the NDB score in two independent cohorts of patients with cervical cancer who had gene expression data, clinical outcomes, and information on treatment received [25,26]. Although the number of patients was small, NDB score was higher in NDB patients than in DCB patients (**Fig. 3D and E**). Furthermore, we observed a significantly lower survival in patients with high NDB scores than in those with low NDB scores in one cohort and a borderline significance of the NDB score in another cohort (**Fig. 3D and E**).

4. Enriched immune-suppressive cells in NDB patients

We next investigated the tumor immune microenvironment in the TCGA-CESC cohort according to the NDB score. The wound healing process that is related to EMT is also an immunologic process involving immune-suppressive cells, such as CAFs, TAMs, and MDSCs [29,30]. Considering the enrichment of the wound healing signature in NDB patients, we evaluated TGF-β response, CAF, TAM, and MDSC signature scores. Indeed, patients with high NDB scores had significantly higher TGF-β response, CAF, TAM, and MDSC signature scores (**Fig. 4A**). Moreover, deconvolution of cell subsets revealed a significant enrichment of CAFs in patients with high NDB scores (**Fig. 4B**). Additionally, a significantly higher proportion of endothelial cells was observed in patients with high NDB scores than in those with low NDB scores (**Fig. 4B**).

5. High NDB scores may associate with poor response to immune checkpoint blockade

Considering the role of immune-suppressive cells in abrogating the effectiveness of ICIs [31], we next investigated the potential of NDB and DCB patients to respond to ICIs. T cell-inflamed GEP [27], which has been shown to predict responses to anti-PD-1 therapy in multiple types of cancer, was found to be significantly enriched in DCB patients (**Fig. 5A**). In the TCGA-CESC cohort, the T cell-inflamed GEP score was higher in patients with low NDB scores than in those with high NDB scores ($p<0.0001$; **Fig. 5B**). However, the neoantigen number, which is also known to be a predictive marker for anti-PD-1 therapy [32], was similar between patients with high and low NDB scores (**Fig. 5C**). Next, we estimated the TIDE score for each patient to predict the probability of responding to ICIs [28]. A lower TIDE score indicated a higher probability of responding to ICIs. The TIDE score was significantly lower

https://doi.org/10.3802/jgo.2022.33.e7

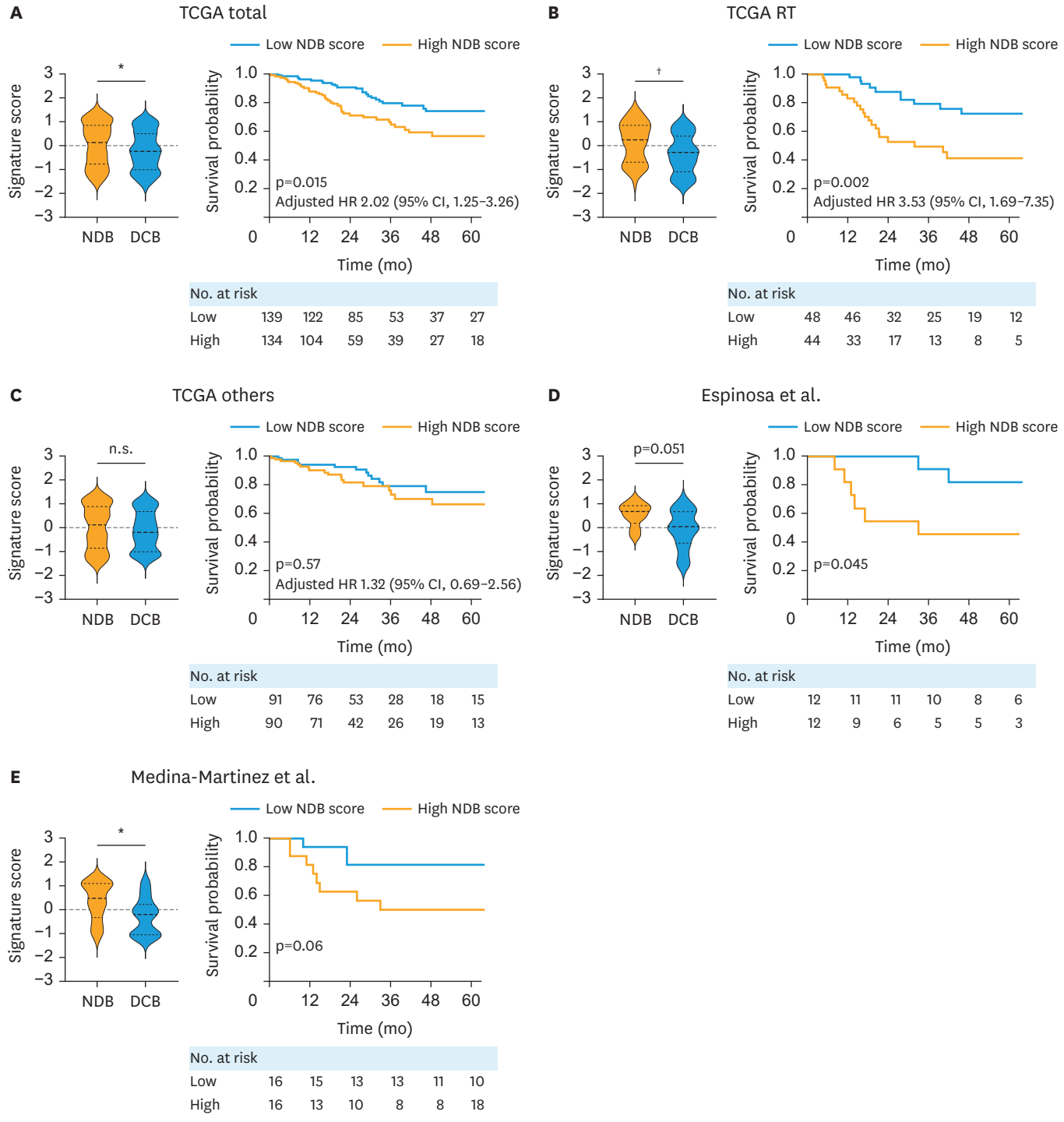

Fig. 3. Predictive value of the NDB score in three independent cohorts of patients with cervical cancer who received curative aim RT. (A-E) Comparison of NDB score in NDB and DCB patients and overall survival patients with cervical cancer according to the NDB score in the TCGA cohort (n=273; A), patients who received curative aim RT (TCGA RT cohort; n=92; B), and those that did not receive curative aim RT (TCGA others; n=181; C). Patients were dichotomized into "high" (NDB score >0) and "low" (NDB score <0) groups. The hazard ratio of the NDB scores was adjusted for age, pathology, and FIGO tumor stage. (D and E) The predictive value of NDB score in two independent cohorts of patients; Espinosa et al. [25] cohort (n=24; D) and Medina-Martinez et al. [26] cohort (n=32; E). CI, confidence interval; DCB, durable clinical benefit; HR, hazard ratio; NDB, no durable benefit; RT, radiotherapy; TCGA, the Cancer Genome Atlas.
*p<0.05; †p<0.01; n.s., not significant.

https://doi.org/10.3802/jgo.2022.33.e7

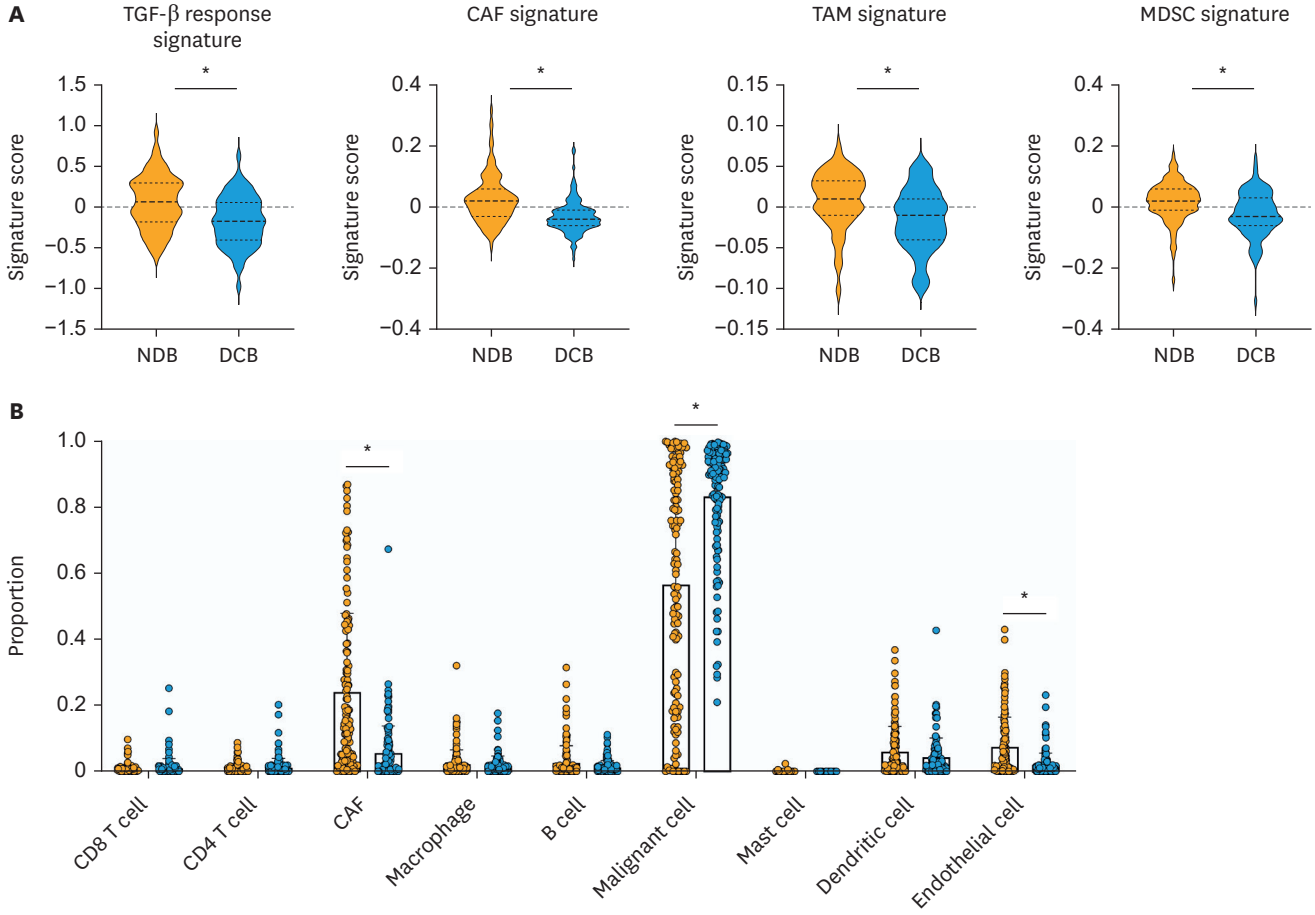

Fig. 4. Gene signatures and cell subtypes enriched in patients with high NDB scores in the TCGA-CESC cohort. (A) Enrichment scores of TGF-β response, CAF, TAM, MDSC gene sets in NDB (n=139; high NDB score) and DCB patients (n = 134; low NDB score) in the TCGA-CESC cohort. (B) Deconvolution of cell subsets in the tumor microenvironment of NDB and DCB patients in the TCGA-CESC cohort.
CAF, cancer-associated fibroblast; DCB, durable clinical benefit; MDSC, myeloid-derived suppressor cell; NDB, no durable benefit; TAM, tumor-associated macrophage; TGF, transforming growth factor; TCGA-CESC, the Cancer Genome Atlas Cervical Squamous Cell and Endocervical Adenocarcinoma.
*p<0.0001.

in patients with a low NDB score than in those with a high NDB score (**Fig. 5D**). Furthermore, significantly more patients with low NDB scores had a TIDE score <0 than those with high NDB scores (59.7% vs. 21.6%; p<0.001; **Fig. 5E**).

DISCUSSION

In the present study, we found that NDB patients exhibited a distinct gene signature that could predict treatment outcomes following CCRT in patients with locally advanced cervical cancer. Using the DEGs between NDB and DCB patients, we estimated the NDB scores for each patient. The NDB score specifically predicted treatment outcome in patients treated with RT but not in those treated with surgery, thus implying that this gene signature is predictive of CCRT responses rather than prognosis. In addition, we discovered key pathways related to the responsiveness to CCRT. Poor responders tended to have upregulated EMT, wound healing, and TGF-β response signatures. Moreover, immune-suppressive cells such as CAFs were enriched in tumors that responded poorly to CCRT. Patients anticipated to have a poor response to CCRT were also less likely to respond to ICIs. These results suggest novel

https://doi.org/10.3802/jgo.2022.33.e7

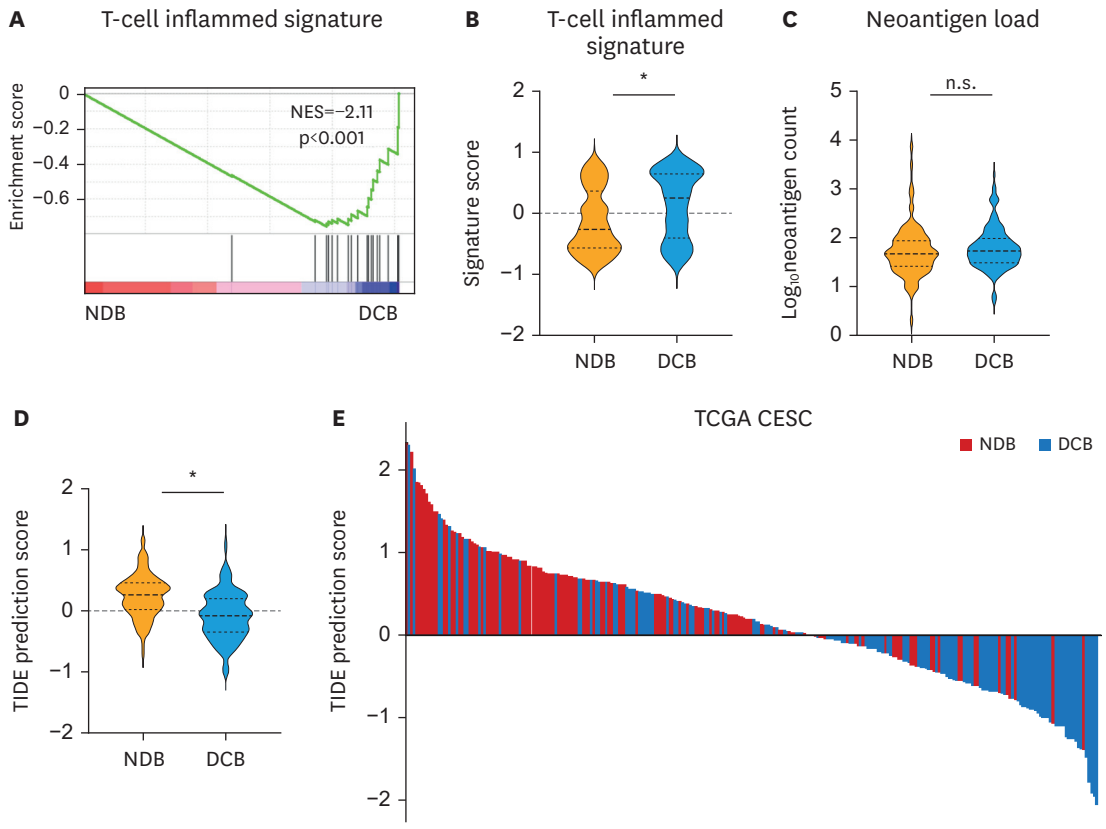

Fig. 5. Patients with high NDB scores are less likely to respond to programmed death-1 blockade. (A) Gene set enrichment analysis of the T-cell inflamed signature in DCB (n=5) and NDB (n=4) patients in our cohort. (B) The signature score of the T-cell inflamed gene set of NDB (high NDB score) and DCB patients (low NDB score) in the TCGA CESC cohort. (C) Neoantigen load, including the single nucleotide variant and indel neoantigens. (D) The mean value of the TIDE prediction score in NDB (high NDB score) and DCB patients (low NDB score). (E) Waterfall plot of the TIDE prediction score in each individual of the TCGA-CESC cohort. NDB (high NDB score) and DCB patients (low NDB score) are denoted in red and blue, respectively.
DCB, durable clinical benefit; NDB, no durable benefit; NES, normalized enrichment score; TIDE, tumor immune dysfunction and exclusion; TCGA-CESC, the Cancer Genome Atlas Cervical Squamous Cell and Endocervical Adenocarcinoma.
*p<0.0001, n.s., not significant.

combinatorial targets, other than ICIs, in patients with cervical cancer that are less likely to be cured by CCRT.

Currently, no predictive biomarker is available to predict outcomes following CCRT for locally advanced cervical cancer. Previously, a gene-expression-based radiosensitivity prediction model was developed from microarray-based gene expression data and surviving fractions at 2 Gy in 48 cancer cell lines [33]. This model successfully predicted outcomes in patients with breast cancer, lung cancer, glioblastoma, and pancreatic cancer [14]. Since this model has been derived from cancer cell lines, it only predicts the intrinsic radiosensitivity of cancer cells. However, the response to RT is not only determined by the radiosensitivity of cancer cells but also by the surrounding tumor microenvironment [34]. In our study, we utilized tumor tissue from patients treated with CCRT that also included the tumor microenvironment. Therefore, the gene signature derived from our study may have better clinical implications for predicting the response to CCRT than the previous model. Moreover, we took advantage of in silico analysis to assess the components of the tumor microenvironment from bulk RNA sequencing data and compared the distribution of the cell subtypes according to treatment response.

https://doi.org/10.3802/jgo.2022.33.e7

We found that the genes upregulated in NDB patients were associated with ECM organization and EMT, whereas genes upregulated in DCB patients were associated with interferon signaling pathways. Moreover, we found enrichment of the TGF-β response signature in patients with NDB, which led us to focus on CAFs. In our study, we also found that the frequency of CAFs in the tumor microenvironment was significantly higher in NDB patients than in DCB patients. Indeed, the proportion of CAFs was also significantly high in patients with high NDB scores in the large TCGA-CESC cohort. CAFs are one of the central components of the ECM organization and EMT. CAFs reprogram the tumor immune microenvironment through the secretion of ECM proteins and multiple types of cytokines such as TGF-β [35]. They also produce ECM-degrading proteases, such as matrix metalloproteinases, and promote EMT and invasiveness of cancer cells. Cancer cells that have undergone EMT acquire properties that enable them to move and reach distant organs [35]. Clinically, half of the patients with recurrent cervical cancer after CCRT present with distant metastasis [5]. To reduce such recurrences, adjuvant chemotherapy following CCRT has been tested in several trials, including the OUTBACK trial (NCT01414608). However, CAFs are also involved in the resistance to chemotherapy; hence, poor responders to CCRT may not benefit much from this strategy. Previous studies have demonstrated conflicting results regarding the efficacy of adjuvant chemotherapy following standard CCRT [8-10]. To further improve outcomes, CAF-directed therapies may be an appealing strategy for poor responders to CCRT. Many clinical trials are investigating diverse approaches for targeting CAFs, including TGF-β inhibitors, fibroblast growth factor receptor inhibitors, and fibroblast activation protein-directed therapies [36].

In addition to CAFs, various gene signatures of other suppressive immune cells, such as TAM and MDSCs, were enriched in patients with high NDB scores. Considering the suppressive tumor immune microenvironment in NDB patients, we further evaluated whether the response to CCRT may be associated with the response to ICIs. We applied established gene expression-based prediction scores for anti-PD-1 therapy [27,28]. DCB patients were enriched for T-cell inflamed gene signatures and had a low TIDE prediction score, which implies that these patients are more likely to respond to anti-PD-1 than NDB patients. Currently, ICIs are actively being tested for locally advanced cervical cancer in conjunction with CCRT. The CALLA (NCT03830866) and KEYNOTE-A18 (NCT04221945) trials are investigating the role of adding durvalumab and pembrolizumab, respectively, during CCRT and after completion of CCRT. In our study, NDB patients exhibited signatures of poor response to anti-PD-1 therapy. However, T cell-inflamed GEP and TIDE prediction score did not include patients with cervical cancer when they were developed and therefore, the predicted poor responses to ICIs in NDB patients should be interpreted carefully. The results from clinical trials are awaited to confirm the benefit of adding anti-PD-1 to standard CCRT.

The present study has several limitations, including the small number and quite heterogeneous baseline characteristics of patients who underwent RNA sequencing. The small number of patients can lead to inappropriate interpretation and limit the conclusions. However, we attempted to externally validate our gene signature in a large cohort and in other independent cohorts. Another limitation is that the histological type is mostly squamous cell carcinoma with a single case of adenocarcinoma. The NDB patient with adenocarcinoma was clustered with the other NDB patients with squamous cell carcinoma. Further studies with a larger number of patients are required to investigate whether poor responders with adenocarcinoma may have a different transcriptome landscape than those with squamous cell carcinoma.

https://doi.org/10.3802/jgo.2022.33.e7

In conclusion, we found that poor responders to CCRT or RT have a distinct GEF; we also describe a novel gene signature that predicts the response to CCRT or RT in locally advanced cervical cancer. Moreover, we demonstrated differences in the tumor microenvironment of poor responders compared to that of favorable responders, such as a high proportion of CAFs and an upregulated EMT signature. Our data also suggest that current treatment strategies may not be efficient in improving treatment outcomes of poor responders to CCRT or RT and that novel treatment combinations should be further investigated.

SUPPLEMENTARY MATERIALS

Table S1

Baseline characteristics of the cohort before and after propensity score matching

Click here to view

Table S2

Differentially expressed genes between NDB and DCB tumors

Click here to view

REFERENCES

1. Sung H, Ferlay J, Siegel RL, Laversanne M, Soerjomataram I, Jemal A, et al. Global cancer statistics 2020: GLOBOCAN estimates of incidence and mortality worldwide for 36 cancers in 185 countries. CA Cancer J Clin 2021;71:209-49.
   PUBMED | CROSSREF
2. Marth C, Landoni F, Mahner S, McCormack M, Gonzalez-Martin A, Colombo N, et al. Cervical cancer: ESMO Clinical Practice Guidelines for diagnosis, treatment and follow-up. Ann Oncol 2017;28:iv72-83.
   PUBMED | CROSSREF
3. Chuang LT, Temin S, Camacho R, Dueñas-Gonzalez A, Feldman S, Gultekin M, et al. Management and care of women with invasive cervical cancer: American Society of Clinical Oncology Resource-Stratified Clinical Practice Guideline. J Glob Oncol 2016;2:311-40.
   PUBMED | CROSSREF
4. National Comprehensive Cancer Network. Cervical Cancer (Version 1.2021) [Internet]. Plymouth Meeting, PA: National Comprehensive Cancer Network; 2021 [cited 2021 Apr 1]. Available from: https://www.nccn.org/professionals/physician_gls/pdf/cervical.pdf.
5. Tan LT, Pötter R, Sturdza A, Fokdal L, Haie-Meder C, Schmid M, et al. Change in patterns of failure after image-guided brachytherapy for cervical cancer: analysis from the RetroEMBRACE study. Int J Radiat Oncol Biol Phys 2019;104:895-902.
   PUBMED | CROSSREF
6. Kim J, Cho Y, Kim N, Chung SY, Kim JW, Lee IJ, et al. Magnetic resonance imaging-based validation of the 2018 FIGO staging system in patients treated with definitive radiotherapy for locally advanced cervix cancer. Gynecol Oncol 2021;160:735-41.
   PUBMED | CROSSREF
7. Vora C, Gupta S. Targeted therapy in cervical cancer. ESMO Open 2019;3 Suppl 1:e000462.
   PUBMED | CROSSREF
8. Dueñas-González A, Zarbá JJ, Patel F, Alcedo JC, Beslija S, Casanova L, et al. Phase III, open-label, randomized study comparing concurrent gemcitabine plus cisplatin and radiation followed by adjuvant gemcitabine and cisplatin versus concurrent cisplatin and radiation in patients with stage IIB to IVA carcinoma of the cervix. J Clin Oncol 2011;29:1678-85.
   PUBMED | CROSSREF

9. Tang J, Tang Y, Yang J, Huang S. Chemoradiation and adjuvant chemotherapy in advanced cervical adenocarcinoma. Gynecol Oncol 2012;125:297-302.
PUBMED | CROSSREF
10. Tangjitgamol S, Tharavichitkul E, Tovanabutra C, Rongsriyam K, Asakij T, Paengchit K, et al. A randomized controlled trial comparing concurrent chemoradiation versus concurrent chemoradiation followed by adjuvant chemotherapy in locally advanced cervical cancer patients: ACTLACC trial. J Gynecol Oncol 2019;30:e82.
PUBMED | CROSSREF
11. Da Silva DM, Enserro DM, Mayadev JS, Skeate JG, Matsuo K, Pham HQ, et al. Immune activation in patients with locally advanced cervical cancer treated with ipilimumab following definitive chemoradiation (GOG-9929). Clin Cancer Res 2020;26:5621-30.
PUBMED | CROSSREF
12. Dyer BA, Feng CH, Eskander R, Sharabi AB, Mell LK, McHale M, et al. Current status of clinical trials for cervical and uterine cancer using immunotherapy combined with radiation. Int J Radiat Oncol Biol Phys 2021;109:396-412.
PUBMED | CROSSREF
13. Sparano JA, Gray RJ, Makower DF, Pritchard KI, Albain KS, Hayes DF, et al. Adjuvant chemotherapy guided by a 21-gene expression assay in breast cancer. N Engl J Med 2018;379:111-21.
PUBMED | CROSSREF
14. Scott JG, Berglund A, Schell MJ, Mihaylov I, Fulp WJ, Yue B, et al. A genome-based model for adjusting radiotherapy dose (GARD): a retrospective, cohort-based study. Lancet Oncol 2017;18:202-11.
PUBMED | CROSSREF
15. Zhao SG, Chang SL, Spratt DE, Erho N, Yu M, Ashab HA, et al. Development and validation of a 24-gene predictor of response to postoperative radiotherapy in prostate cancer: a matched, retrospective analysis. Lancet Oncol 2016;17:1612-20.
PUBMED | CROSSREF
16. Kim KH, Kim S, Kim GE, Koom WS, Kim SW, Nam EJ, et al. De-escalation of the cumulative central radiation dose according to the tumor response can reduce rectal toxicity without compromising the treatment outcome in patients with uterine cervical cancer. Gynecol Oncol 2015;139:439-46.
PUBMED | CROSSREF
17. Huang W, Sherman BT, Lempicki RA. Systematic and integrative analysis of large gene lists using DAVID bioinformatics resources. Nat Protoc 2009;4:44-57.
PUBMED | CROSSREF
18. Thorsson V, Gibbs DL, Brown SD, Wolf D, Bortone DS, Ou Yang TH, et al. The immune landscape of cancer. Immunity 2019;51:411-2.
PUBMED | CROSSREF
19. Mak MP, Tong P, Diao L, Cardnell RJ, Gibbons DL, William WN, et al. A patient-derived, pan-cancer EMT signature identifies global molecular alterations and immune target enrichment following epithelial-to-mesenchymal transition. Clin Cancer Res 2016;22:609-20.
PUBMED | CROSSREF
20. Kim HS, Kim SC, Kim SJ, Park CH, Jeung HC, Kim YB, et al. Identification of a radiosensitivity signature using integrative metaanalysis of published microarray data for NCI-60 cancer cells. BMC Genomics 2012;13:348.
PUBMED | CROSSREF
21. Newman AM, Steen CB, Liu CL, Gentles AJ, Chaudhuri AA, Scherer F, et al. Determining cell type abundance and expression from bulk tissues with digital cytometry. Nat Biotechnol 2019;37:773-82.
PUBMED | CROSSREF
22. Calon A, Espinet E, Palomo-Ponce S, Tauriello DV, Iglesias M, Céspedes MV, et al. Dependency of colorectal cancer on a TGF-β-driven program in stromal cells for metastasis initiation. Cancer Cell 2012;22:571-84.
PUBMED | CROSSREF
23. Beyer M, Mallmann MR, Xue J, Staratschek-Jox A, Vorholt D, Krebs W, et al. High-resolution transcriptome of human macrophages. PLoS One 2012;7:e45466.
PUBMED | CROSSREF
24. Yaddanapudi K, Rendon BE, Lamont G, Kim EJ, Al Rayyan N, Richie J, et al. MIF is necessary for late-stage melanoma patient MDSC immune suppression and differentiation. Cancer Immunol Res 2016;4:101-12.
PUBMED | CROSSREF

25. Espinosa AM, Alfaro A, Roman-Basaure E, Guardado-Estrada M, Palma Í, Serralde C, et al. Mitosis is a source of potential markers for screening and survival and therapeutic targets in cervical cancer. PLoS One 2013;8:e55975.
PUBMED | CROSSREF
26. Medina-Martinez I, Barrón V, Roman-Bassaure E, Juárez-Torres E, Guardado-Estrada M, Espinosa AM, et al. Impact of gene dosage on gene expression, biological processes and survival in cervical cancer: a genome-wide follow-up study. PLoS One 2014;9:e97842.
PUBMED | CROSSREF
27. Ayers M, Lunceford J, Nebozhyn M, Murphy E, Loboda A, Kaufman DR, et al. IFN-γ-related mRNA profile predicts clinical response to PD-1 blockade. J Clin Invest 2017;127:2930-40.
PUBMED | CROSSREF
28. Jiang P, Gu S, Pan D, Fu J, Sahu A, Hu X, et al. Signatures of T cell dysfunction and exclusion predict cancer immunotherapy response. Nat Med 2018;24:1550-8.
PUBMED | CROSSREF
29. Schwörer S, Vardhana SA, Thompson CB. Cancer metabolism drives a stromal regenerative response. Cell Metab 2019;29:576-91.
PUBMED | CROSSREF
30. Hua Y, Bergers G. Tumors vs. chronic wounds: an immune cell's perspective. Front Immunol 2019;10:2178.
PUBMED | CROSSREF
31. Oliver AJ, Lau PK, Unsworth AS, Loi S, Darcy PK, Kershaw MH, et al. Tissue-dependent tumor microenvironments and their impact on immunotherapy responses. Front Immunol 2018;9:70.
PUBMED | CROSSREF
32. Schumacher TN, Schreiber RD. Neoantigens in cancer immunotherapy. Science 2015;348:69-74.
PUBMED | CROSSREF
33. Eschrich SA, Pramana J, Zhang H, Zhao H, Boulware D, Lee JH, et al. A gene expression model of intrinsic tumor radiosensitivity: prediction of response and prognosis after chemoradiation. Int J Radiat Oncol Biol Phys 2009;75:489-96.
PUBMED | CROSSREF
34. Barker HE, Paget JT, Khan AA, Harrington KJ. The tumour microenvironment after radiotherapy: mechanisms of resistance and recurrence. Nat Rev Cancer 2015;15:409-25.
PUBMED | CROSSREF
35. Kalluri R. The biology and function of fibroblasts in cancer. Nat Rev Cancer 2016;16:582-98.
PUBMED | CROSSREF
36. Sahai E, Astsaturov I, Cukierman E, DeNardo DG, Egeblad M, Evans RM, et al. A framework for advancing our understanding of cancer-associated fibroblasts. Nat Rev Cancer 2020;20:174-86.
PUBMED | CROSSREF